Available online at www.sciencedirect.com
SCIENCE DIRECT®
Journal of Molecular Catalysis A: Chemical 211 (2004) 237–242
JOURNAL OF MOLECULAR CATALYSIS A: CHEMICAL
www.elsevier.com/locate/molcata

Generation of a silica skeleton inside of gel-type functional resins supporting catalytically active palladium nanoclusters

B. Corain [a,*], P. Guerriero [b], G. Schiavon [c], M. Zapparoli [d], M. Kralik [e]

[a] *C.N.R., Sezione di Padova, c/o Dipartimento di Chimica Inorganica Metallorganica Analitica, Istituto di Scienze e Tecnologie Molecolari, Via Marzolo 1, 35131 Padova, Italy*
[b] *C.N.R., Corso Stati Uniti 4, Istituto di Chimica Inorganica e dei Materiali, 35127 Padova, Italy*
[c] *Lehrstuhl für Anorganische und Analitische Chemie, T.U. München, Lichtenberg Strasse 4, D-85747 Garching, Germany*
[d] *C.I.G.S. University Modena, Modena, Italy*
[e] *Department of Organic Technology, Slovak University of Technology, Radlinskeho 9, 812 37 Bratislava 1, Slovak Republic*

Received 5 May 2003; received in revised form 17 October 2003; accepted 18 October 2003

Abstract

Supported Pd catalysts based on Pd^0 nanoclusters that are homogeneously dispersed inside of organic–inorganic nanocomposites, are produced along two different synthetic routes. Pre-formed R/SiO_2 composites (R: functional gel-type resin) are let to react with Pd^{II} in a suitable liquid medium to give $R/SiO_2/Pd^{II}$ materials that are readily transformed into three-components $R/SiO_2/Pd^0$ composites upon reduction with $NaBH_4$. Alternatively, quite similar $R/SiO_2/Pd^0$ materials are obtained upon generating a silica skeleton inside of pre-formed R/Pd^0 two-component composites. Two- and three-component composites are thoroughly characterized with various physico-chemical techniques.

Keywords: Functional gel-type resin; resin/Pd^0/SiO_2; Organic–inorganic nanocomposites

1. Introduction

We have recently reported on the chemical and mechanical stability of resins-supported Pd^0 catalysts, R/Pd^0 (R: functional gel-type resin) that are found to combine satisfactory activity and reusability in the hydrogenation of cyclohexene under mild conditions [1]. We have also recently reported in this Journal on the synthesis, preliminary characterization and catalytic activity of two three-components composites based on a given functional gel-type resin, R, nanoclustered palladium(0), Pd^0, and amorphous silica, SiO_2 [2], i.e. $R/Pd^0/SiO_2$. These catalysts appear to combine reasonable activity, good mechanical and chemical stability and excellent separability from the reaction mixture (re-usability), showing very promising features for technological feasibility.We report here on the synthesis of catalysts $R/Pd^0/SiO_2$ along two different routes:

$$R \rightarrow R/SiO_2 \rightarrow R/Pd^{II}/SiO_2 \rightarrow R/Pd^0/SiO_2 \quad (\text{route } \alpha)$$

and

$$R \rightarrow R/Pd^{II} \rightarrow R/Pd^0 \rightarrow R/Pd^0/SiO_2 \quad (\text{route } \beta)$$

Moreover, we report on the very nature of our composites down to the nanometer scale and we will show that they are in fact organic–inorganic nanocomposites (OINC's). Finally, we will provide clear evidence of the reasons why the generation of a silica skeleton inside of the nanoporous domains of the hosting gel-type functional resins does not severely damp their catalytic activity when compared with their R/Pd^0 analogs [2].

Organic–inorganic nanocomposites (OINC's) are actively investigated materials as shown by recent literature [3]. Their crucial feature is the co-existence of inorganic and organic entities in space volumes as small as tens or hundreds of cubic nanometers in size. The extreme proximity (and mutual entanglement) of their individual frameworks produces materials with peculiar, possibly synergistic, properties compared with those of the (macro)molecular components.

These materials are typically prepared from an inorganic pre-existing framework that behaves either as a template for the generation of an organic framework inside of it [4], or more simply, as a hosting porous spectator able to

* Corresponding author. Tel.: +39-049-8275211; fax: +39-049-8275223/8255161.
E-mail address: benedetto.corain@unipd.it (B. Corain).

1381-1169/$ – see front matter © 2003 Elsevier B.V. All rights reserved.
doi:10.1016/j.molcata.2003.10.029

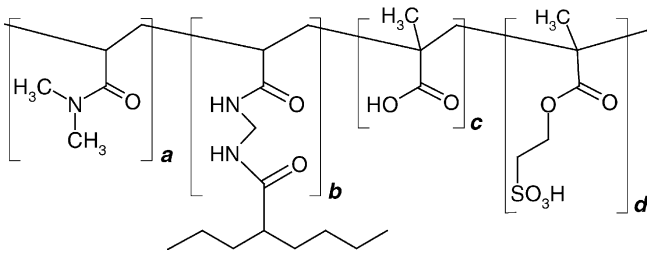

Fig. 1. A sketch of the structure of SPIM(H) and MPIF(H) materials; *a*, *b*, *c* and *d* are equal to (mol.%) 92, 4, 0, 4 and 88, 4, 8, 0 for SPIM(H) and MPIF(H), respectively.

adsorb pre-formed organic polymers [5,6]. In other cases OINC's are obtained upon controlled polycondensation of Si^{IV}-based "organic" monomers [7] or upon generating a silica framework in the presence of tetralkylammonium ion pairs-stabilized metal nanoclusters [8] or upon pre-forming an essentially silica-like framework that contains (photo)polymerizable carbon–carbon double bonds [9]. We mention also the cases of OINC's generation via sol–gel polycondensation of inorganic precursors in the presence of highly ordered metallo-organic molecular structures [10] and the production of a silica skeleton inside of the macropores of strongly basic Dowex MSA-1 resins [11] and of the macropores of porous Amersham Biosciences organic beads [12].

We report in this paper on the synthesis of OINC's materials that resemble those mentioned in [11,12] but that result from the generation of SiO_2 inside of the micropores (in fact nanopores [13–16]) of functional resins of the gel-type.

In order to be coherent in this paper with previous codings used in our related papers, we introduce a coding that stems from Fig. 1. Functional gel-type resins are SPIM(H) and MPIF(H) in their protonated, as prepared, form and in the form of $SPIM^-Na^+$ [1] and $MPIF^-Na^+$ when they stem from the reduction step that is implicated in both routes α and β, Fig. 1 [1,17]. The herein described morphological analysis at the nanometer level will provide clear evidence of the reasons that permit the attainment of quite acceptable catalytic activity in materials that stem from the merging of the accessible frameworks of two active conventional catalysts such as $SPIM^-Na^+/Pd^0$ and $MPIF^-Na^+/Pd^0$ [1] with the framework of amorphous silica designed to be, in this case, just a spectator filler.

2. Results and discussion

2.1. Route α

Resins SPIM(H) and MPIF(H) are impregnated with a partially hydrolyzed methanol solution of TEOS (see Section 4) to give eventually materials that from the relevant thermogravimetric analysis (Table 1) do appear to contain an inorganic component, coexisting with an organic, thermodegradable one, i.e. $SPIM(H)/SiO_2$ and $MPIF(H)/SiO_2$, respectively. Picnometric density measurements provide further indirect support to this view. Thus, density values equal to 1.12 and 1.05 g/ml observed for MPIF(H) and SPIM(H) become 1.24 and 1.14 g/ml, respectively, in the corresponding resin/silica composites.

The scope of the synthesized organic–inorganic composites is illustrated in Table 1.

It is seen that the organic–inorganic-Pd composites are nicely obtained upon starting from pre-formed resin–silica composites and from pre-formed resin–Pd composites. In this connection, remarkable is the observation that both $SPIM(H)/SiO_2$ and $MPIF(H)/SiO_2$ are found to exhibit a marked bonding ability towards Pd^{II} leading to the quantitative incorporation of the metal centre, expectedly attributable to the organic component of the composites [20]. This observation reveals a substantial independence of the bonding ability of the trapping component (the functional resin) of the physical presence of the trapped silica skeleton. This finding is remarkable in that our ISEC data (see below) do unambigously reveal that the mutual entanglement of the SPIM(H) and the SiO_2 skeletons occurs down to the nanometer scale so that the composites herein described are to be considered real interpenetrating polymer networks, i.e. IPN materials [18] and conceptually different, albeit related, from those described in [11,19], where the interpenetration is likely to occur at the micrometer level (i.e. thanks to the availability of pre-existing macropores).

SEM analysis of $SPIM(H)/SiO_2$ and $MPIF(H)/SiO_2$ does not show any morphological change in comparison with the

Table 1
Production and features of $SPIM(H)/SiO_2$, $MPIF(H)/SiO_2$, α-$SPIM^-Na^+/Pd^0/SiO_2$, α-$MPIF^-Na^+/Pd^0/SiO_2$, β-$SPIM^-Na^+/Pd^0/SiO_2$ β-$MPIF^-Na^+/Pd^0/SiO_2$ (see text and Table 2)

Entry	Code	SiO_2[a] (%)	Pd (%)	Production
1	$SPIM(H)/SiO_2$	21	–	From SPIM(H) + TEOS
2	$MPIF(H)/SiO_2$	27	–	From MPIF(H) + TEOS
3	α-$SPIM^-Na^+/Pd^0{\cdot}SiO_2$	–	1.00[b]	From $SPIM(H)/SiO_2$ + Pd^{II}
4	α-$MPIF^-Na^+/Pd^0{\cdot}SiO_2$	–	0.96[b]	From $MPIF(H)/SiO_2$ + Pd^{II}
5	β-$SPIM^-Na^+/Pd^0{\cdot}SiO_2$	22	1.30	From $SPIM^-Na^+/Pd^0$ + TEOS
6	β-$MPIF^-Na^+/Pd^0{\cdot}SiO_2$	30	1.91	From $MPIF^-Na^+/Pd^0$ + TEOS

[a] Determined from TGA under air.
[b] Quantitative incorporation of Pd^{II} (see text).

Table 2
ISEC analysis of SPIM(H), MPIF(H), SPIM(H)/SiO_2 and MPIF(H)/SiO_2

Polymer chain concentration (nm/nm^3)	Volume fractions of gel phase (V_i, ml/g)			
	SPIM(H)	SPIM(H)/SiO_2	MPIF(H)	MPIF(H)/SiO_2
0.1	0.0	0.0	0.1	0.0
0.2	2.9	0.1	0.2	0.2
0.4	0.9	0.8	1.8	0.0
0.8	0.0	0.0	0.0	0.0
1.5	0.0	0.7	0.0	1.2
ΣV_i (ml/g)[a]	3.0	1.6	2.1	1.4
$V_{totalgel}$ (ml/g)[b]	3.5	2.3	2.2	2.0

[a] Total gel volume "seen" by ISEC molecular probe *s*.
[b] Total gel volume including that inaccessible even to the smallest ISEC molecular probe (e.g. D_2O).

hosting matrices. On the contrary, as expected, XRMA of sections of particles of the two composites exhibits a thorough homogeneous distribution of silicon in the body of the composites particles. It has to be stressed that, in the light of the expected lateral resolution power of XRMA (ca. 5 μm), the observed homogeneity does not support per se an interpenetration of the host and guest frameworks at a nanometric (i.e. at a (macro)molecular) level. This crucial feature will be in fact demonstrated by ISEC analysis in water (Table 2 and Fig. 2) [16,19].

Inspection of Table 2 reveals that resins nanoporosity is mainly featured by 0.2 and 0.4 nm^{-2} domains in both SPIM(H) and MPIF(H) that correspond to the domains built-up with ca. 3 nm "cylindrical pores" [17,19]. Apparently, most of these domains disappear with the formation of both composites, especially in the case of MPIF(H)/SiO_2, in which mainly 1.5 nm^{-2} (ca. 0.6 nm pores) domains are featuring its polymer framework. A related situation is seen for SPIM(H)/SiO_2, in which 2.8 ml/g low chain density domains (0.2 nm^{-2}) disappear out of 2.9 ml/g existing ones in the host matrix. An obvious conclusion stemming from these observations is that the generation of the guest silica framework in both composites must occur inside of the less dense domains of the hosting matrix. Consequently, the resulting IPN material is such down to the very nanometric scale, i.e. to the (macro)molecular level. And yet, in spite of this extreme mutual entanglement of two quite different frameworks, the organic component appears to maintain its major chemical property, i.e. ion exchange capacity. Indeed, SPIM(H)/SiO_2 and MPIF(H)/SiO_2, reacting with $Pd(OAc)_2$ in THF:water 2:1, do incorporate the amount of Pd^{II} that is expected from the molar fraction of the acidic component present in the OINC's [20]. Subsequent reduction of Pd^{II} to Pd^0 is also observed as for normal resin–Pd^{II} materials [20]. XRMA of α-SPIM$^-Na^+/Pd^0 \cdot SiO_2$ and of α-MPIF$^-Na^+/Pd^0 \cdot SiO_2$ reveal the expected homogeneous dispersion of palladium through the body of the composites particles (within the limits connected with the 5 μm lateral resolution power of XRMA).

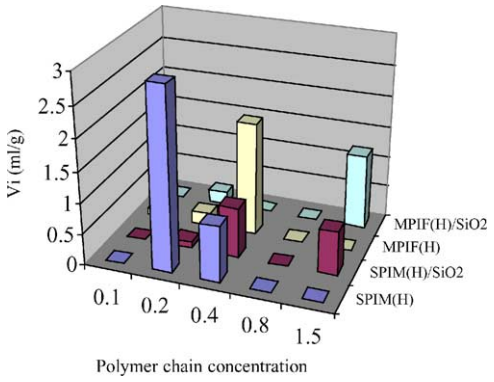

Fig. 2. ISEC analysis of SPIM(H), MPIF(H), SPIM(H)/SiO_2 and MPIF(H)/SiO_2.

The whole of these data appear to offer a rather detailed decription of our resin–silica composites, with a particular emphasis on the persisting molecular accessibility of the organic component inside of which the catalytically active Pd nanoclusters are generated and consequently located.

2.2. Route β

As anticipated in the introductory part of this paper, we became interested to apply the rationale and the results depicted so far to a couple of resin/Pd^0 catalysts, SPIM$^-Na^+/Pd^0$ [1] and MPIF$^-Na^+/Pd^0$ [17] that belong to an extensive group of resin/Pd^0 materials, which we extensively investigated as carefully designed catalysts in the last decade [20].

SPIM$^-Na^+/Pd^0$ and MPIF$^-Na^+/Pd^0$ are black materials that are impregnated with a partially hydrolyzed TEOS solution ethanol at ca. 20 °C and the generation of silica is let to occur in 48 h at 20 °C, exactly as in the case of SPIM(H) and MPIF(H). The final products, β-SPIM$^-Na^+/Pd^0/SiO_2$ and β-MPIF$^-Na^+/Pd^0/SiO_2$ are black materials featured by the properties described below. The transformation of MPIF$^-Na^+/Pd^0$ into β-MPIF$^-Na^+/Pd^0/SiO_2$ is accompanied by a massive increase of weight (1.5 g of MPIF$^-Na^+/Pd^0$ turns out to be transformed into 2.3 g of β-MPIF$^-Na^+/Pd^0/SiO_2$) but no morphological changes are seen to be associated with composite generation (SEM control).

β-SPIM$^-Na^+/Pd^0/SiO_2$ undergoes extensive thermodecomposition from 350 to 600 °C with a weight loss of 78%. β-MPIF$^-Na^+/Pd^0/SiO_2$ behaves quite similarly with a loss of 70%. It is apparent that a substantial fraction of the frameworks of β-SPIM$^-Na^+/Pd^0/SiO_2$ and of β-MPIF$^-Na^+/Pd^0/SiO_2$ is thermally stable up to 600 °C as expected in the presence of a silica skeleton.

SPIM$^-Na^+/Pd^0$ and in particular β-MPIF$^-Na^+/Pd^0/SiO_2$ exhibit a quite homogeneous distribution of both Pd and Si in their XRMA scanning pictures (resolution power is ca. 5 μm) referring to the cross-section of a material particle (Fig. 2). The material obtained after heating β-MPIF$^-Na^+/Pd^0/SiO_2$ up to 600 °C (heating rate equal to

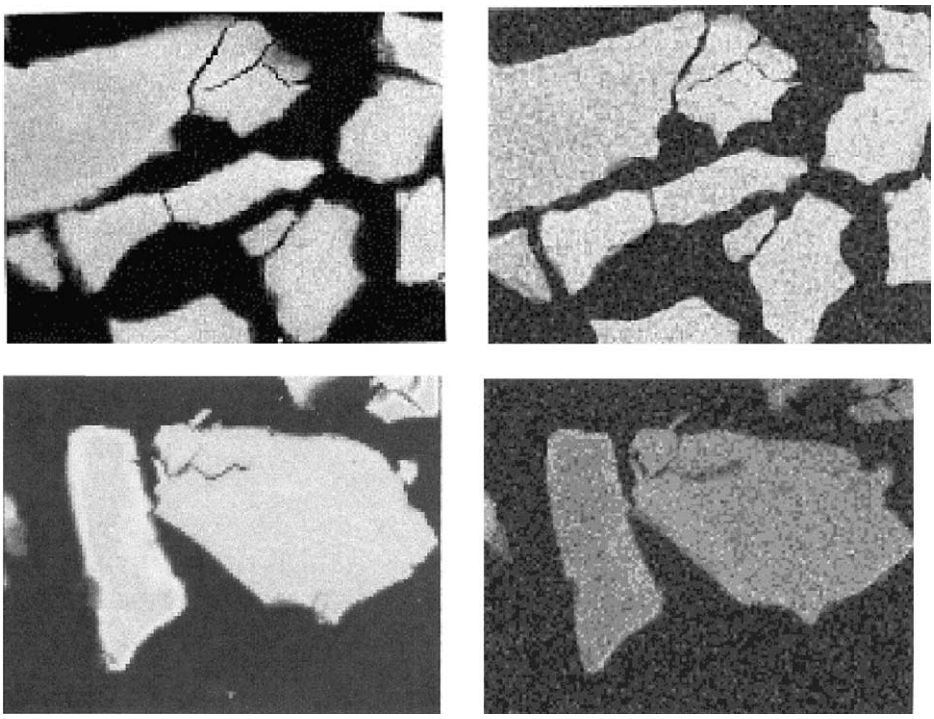

Fig. 3. (Upper figure) XRMA maps for silicon (left) and palladium (right) for β-MPIF^{-}Na^{+}/Pd^{0}/SiO$_2$ (particles: 180–400 μm) and (lower figure) for MPIF^{-}Na^{+}/Pd^{0}/SiO$_2$·Δ.

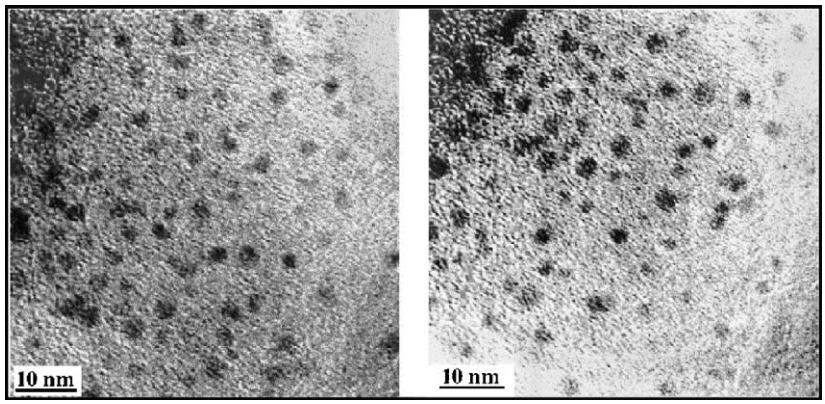

Fig. 4. Low resolution TEM picture of MPIF^{-}Na^{+}/Pd^{0} (left) and of MPIF^{-}Na^{+}/Pd^{0}/SiO$_2$·Δ (right).

30 °C/min, under nitrogen) will be hereafter referred to as MPIF^{-}Na^{+}/Pd^{0}/SiO$_2$·Δ.

β-MPIF^{-}Na^{+}/Pd^{0}/SiO$_2$ exhibits a specific swelling (determined from bulk expanded volumes measurements) in methanol, equal to ca. 1.9 cm^3/g, that is just smaller than that exhibited by MPIF^{-}Na^{+}/Pd^{0}, 2.1 cm^3/g, after correction for the presence of the inorganic "guest". Notice the amazing agreement between these rough data and those determined as V_{totalgel} for the as prepared matrix MPIF(H) (2.2) and for the relevant OICN (2.0), from ISEC (Table 2 and Fig. 3).

TEM analysis of MPIF^{-}Na^{+}/Pd^{0}/SiO$_2$·Δ. (Fig. 4) reveals that Pd nanoclusters, known to be 1.9 nm (average) in MPIF^{-}Na^{+}/Pd^{0} [17], appear well distributed and regular in size, 2.3 nm (average), also in the obtained material thus showing that the final inorganic Pd^{0}/SiO$_2$ composite does contain almost monodispersed palladium nanoclusters, the size of which has been conditioned by the *templating action* [17] of the MPIF^{-}Na^{+} polymer framework.

Size distribution analysis of Pd nanoclusters before and after thermal treatment reveals that a reasonable size control is maintained after the severe thermal treatment, with a moderate effect on the average size (see above). The observed moderate increase of nanoclusters size is not unex-

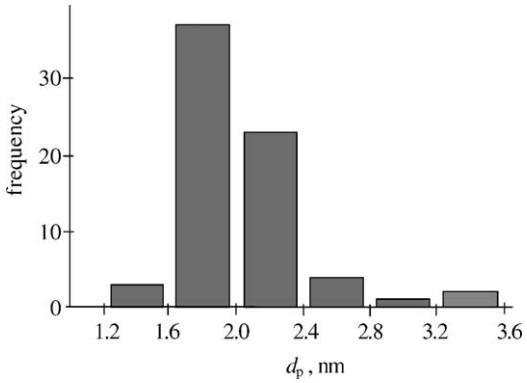

Fig. 5. Size distribution of the palladium nanoclusters of MPIF$^-$Na$^+$/Pd^0 determined by computer image analysis.

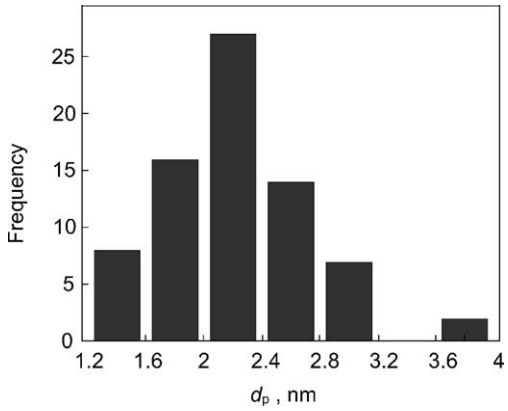

Fig. 6. Size distribution of the palladium nanoclusters of MPIF$^-$Na$^+$/Pd^0·Δ determined by computer image analysis.

pected in the light of a possible appreciable sintering affect Figs. 5 and 6.

3. Conclusions

Swollen gel-type functional resins acting as supports for the homogeneous dispersion of Pd nanoparticles, are found to be effective media for dispersing a sol–gel generated silica skeleton. In the resulting organic–inorganic nanocomposite, the organic and inorganic frameworks appears to be homogeneously interpenetrated down to the nanometer scale. The nanomorphology of the organic component, albeit featured by a modest porosity (Table 2), turns out to be suitable for the diffusion of molecules of substantial size (ISEC and bulk expanded volume measurements), thus fitting our catalytic data reported in [2] (hydrogenation of cyclohexene in ethanol at almost ambient conditions). The perceivable reduction of catalytic activity observed in [2] upon moving from catalysts resin/Pd^0/ to catalysts resin/Pd^0/SiO$_2$ associated with the generation of the inorganic guest component, is now properly understood and turns out to be compensated by the exceedingly facile separability from the reaction mixture of the catalyst to be recycled and by a remarkable mechanical stability. As an interesting aside, it is seen that thermal decomposition of the organic framework does modestly affect size and size dispersion of pre-generated Pd nanoclusters.

4. Experimental

4.1. Apparatuses

SEM and XRMA, Cambridge Stereoscan 250 EDX PW 9800; TGA, Thermogravimetric System Perkin-Elmer; TEM, Jeol 2010 with GIF. ISEC measurements and relevant results have been kindly provided by Dr. K. Jerabek Institute of Chemical Process Fundamentals, Praha. Measurements were carried out using an established procedure and a standard chromatographic set-up described elsewhere [19,21,22]. Samples for TEM analysis were prepared by extensive grinding of the as prepared material to be examined, which was subsequently ultrasonically dispersed in methanol and then transferred as a suspension to a copper grid covered with a lacey carbon film.

4.2. Solvents and chemicals

Solvents and chemicals, from various commercial sources, were of reagent grade and were used as received. Methacryloylethylensulfonate (H^+ form) (called also sulfoethylmethacrylate, SEMA), methacrylic acid (MA), *N*,*N*′-dimethylacrylamide (DMAA) and *N*,*N*′-methylene bisacrylamide (MBAA) were from Polysciences. High purity TEOS was from Aldrich.

4.3. Resins and composites synthesis

SPIM(H), MPIF(H), SPIM$^-$Na$^+$/Pd^0 and MPIF$^-$Na$^+$/Pd^0 were prepared according to [1,17]. SPIM(H)/SiO$_2$ and MPIF(H)/SiO$_2$ are prepared upon reacting 1.5 g of acidic resin with 15 ml of a 1 M solution of TEOS, 4 M water and 10^{-2} M HCl in methanol ("pre-aged" for 24 h under moderate stirring) for 3 h under moderate stirring, at room temperature. The obtained material is recovered upon filtration with a Gooch filter at ambient pressure to obtain a just moistened precipitate that is subjected to the action of a membrane vacuum pump for ca. 20 s, after which time the material is left to stand in the same Gooch filter for 48 h at ambient conditions. At this point, the material is washed with methanol (3 × 20 ml), recovered after pump drying and finally fully dried at 70 °C at 5 Torr up to constant weight. α-SPIM$^-$Na$^+$/Pd^0/SiO$_2$ and α-MPIF$^-$Na$^+$/Pd^0/SiO$_2$ are prepared upon reacting 1.5 g of SPIM(H)/SiO$_2$ and MPIF(H)/SiO$_2$ with 25 mg of Pd(OAc)$_2$ dissolved in 10 ml THF/H$_2$O (2:1). Rapid and complete decoloration of the liquid phase occurs and the so obtained brown material, after filtration and washing with 2:1 THF/H$_2$O (3 × 20 ml), is let to react with NaBH$_4$ (5.3 mmol) in ethanol (40 ml) under moderate stirring. After 30 min, a

black material is obtained (Table 1) that is recovered upon filtration and washed with ethanol (3 × 20 ml). Composites β-SPIM^{-}Na^{+}/Pd^{0}/SiO$_2$ and β-MPIF^{-}Na^{+}/Pd^{0}/SiO$_2$ are prepared exactly as SPIM(H)/SiO$_2$ and MPIF(H)/SiO$_2$ upon starting from SPIM^{-}Na^{+}/Pd^{0} and MPIF^{-}Na^{+}/Pd^{0} [17].

Acknowledgements

We are indebted to Dr. K. Jerabek, Institute of Chemical Process Fundamentals, Rozvojova 135, CR-16502 Suchdol, Praha 6, Czech Republic, for ISEC measurements and for helpful discussion, with Dr. G. Pace, CNR Padova for TGA measurements and with Dr. S. Lora, CNR Padova for the synthesis of functional resins. This work was partially supported by P.R.I.N. funding, 2001–2003, Ministero dell'Università e della Ricerca Scientifica, Italy (Project number 2001038991) and by funds of the Slovak VEGA (Project 1/9142/02).

References

[1] M. Kralik, V. Kratky, M. De Rosso, M. Tonelli, S. Lora, B. Corain, Chem. Eur. J. 9 (2003) 209.
[2] M. Kralik, V. Kratky, P. Centomo, P. Guerriero, S. Lora, B. Corain, J. Mol. Catal. A: Chem. 195 (2003) 219.
[3] P. Gomez-Romero, Adv. Mater. 13 (2001) 1632.
[4] S.B. Yoon, K. Sohn, J.Y. Kim, C.-H. Shin, J.-S. Yu, T. Hyeon, Adv. Mater. 14 (2002) 19.
[5] M.A. Harmer, W.E. Farneth, Q. Sun, J. Am. Chem. Soc. 118 (1996) 7708.
[6] Y.-G. Hsu, L.-C. Tu, K.-H. Lin, J. Polym. Res. 8 (2001) 37.
[7] E. Lindner, S. Brugger, S. Steinbrecher, E. Plies, H.A. Mayer, J. Mater. Chem. 11 (2001) 1393.
[8] M. Retz, M. Dugal, Catal. Lett. 58 (1999) 207.
[9] E. Müh, M. Stieger, J.E. Klee, H. Frey, R. Mülhaupt, J. Polym. Sci. A: Polym. Chem. 39 (2001) 37.
[10] M. Kimura, K. Wada, K. Ohta, K. Hanabusa, H. Shirai, N. Kobayashi, J. Am. Chem. Soc. 123 (2001) 2438.
[11] L. Tosheva, J. Sterte, Chem. Commun. (2001) 1112.
[12] U. Meyer, A. Larsson, H.-P. Hentze, R.A. Caruso, Adv. Mater. 14 (2002) 1768.
[13] A. Biffis, B. Corain, M. Zecca, C. Corvaja, K. Jeràbek, J. Am. Chem. Soc. 117 (1995) 1603.
[14] M. Zecca, A. Biffis, G. Palma, S. Lora, K. Jeràbek, B. Corain, Macromolecules 29 (1996) 4655.
[15] A.A. D'Archivio, L. Galantini, E. Tettamanti, A. Panatta, B. Corain, J. Mol. Catal. A: Chem. 157 (2000) 269.
[16] B. Corain, M. Zecca, K. Jerabek, J. Mol. Catal. A: Chem. 177 (2001) 3.
[17] F. Artuso, A.A. D'Archivio, S. Lora, K. Jerabek, M. Kralik, B. Corain, Chem. Eur. J. 9 (2003) 5292.
[18] L.H. Sperling, Chemtech 104 (1998).
[19] K. Jeràbek, in: M. Potschka, P.L. Dubin (Eds.), Cross Evaluation of Strategies in Size-Exclusion Chromatography, ACS Symposium Series 635, American Chemical Society, Washington, DC, USA, 1996, pp. 211.
[20] B. Corain, M. Kralik, J. Mol. Catal. A: Chem. 173 (2001) 99, and references therein.
[21] K. Jerabek, Anal. Chem. 57 (1988) 1598.
[22] K. Jerabek, K. Setinek, Polym. Sci. A: Polym. Chem. 28 (1990) 1387.